energies

MDPI

Article

Impacts of Natural Gas Pipeline Congestion on the Integrated Gas–Electricity Market in Peru

Richard Navarro [1], Hugo Rojas [1], Jaime E. Luyo [1], Jose L. Silva [2] and Yuri P. Molina [2,*]

[1] Faculty of Mechanical Engineering, National University of Engineering, Lima 15333, Peru; richard.navarro.r@uni.pe (R.N.); hrojase@uni.pe (H.R.); jeluyo@yahoo.es (J.E.L.)
[2] Department of Electrical Engineering, Federal University of Paraíba, João Pessoa 58051-900, Paraíba, Brazil; joseleandro.silva@estudante.cear.ufpb.br
* Correspondence: molina.rodriguez@cear.ufpb.br

Abstract: This paper investigates the impact of natural gas pipeline congestion on the integrated gas–electricity market in Peru, focusing on short-term market dynamics. By simulating congestion by reducing the primary natural gas pipeline's capacity, the study reveals significant patterns in production costs and load flows within the electrical network. The research highlights the critical interdependencies between natural gas and electricity systems, emphasizing how constraints in one network can directly affect the other. The findings underscore the importance of coordinated management of these interconnected systems to optimize economic dispatch and ensure the reliability of both gas and electricity grids. The study also proposes strategic public policy interventions to mitigate the financial and physical impacts of pipeline congestion, contributing to more efficient and resilient energy market operations.

Keywords: economic dispatch; electricity grid; gas grid; natural gas; thermal power stations; optimization

Citation: Navarro, R.; Rojas, H.; Luyo, J.E.; Silva, J.L.; Molina, Y.P. Impacts of Natural Gas Pipeline Congestion on the Integrated Gas–Electricity Market in Peru. *Energies* **2024**, *17*, 4586. https://doi.org/10.3390/en17184586

Academic Editor: George Halkos

Received: 14 August 2024
Revised: 30 August 2024
Accepted: 6 September 2024
Published: 12 September 2024

1. Introduction

Despite the traditionally well-defined interconnection between electricity and gas networks, these infrastructures have typically been managed as separate systems. However, it is crucial to acknowledge the vital role of gas-fired generators in electricity production, as highlighted in recent research [1]. Moreover, with the increasing need to balance the variability of renewable energy sources and the potential of green hydrogen for decarbonizing the energy sector, a significant shift is occurring, as detailed in [2]. This shift marks a major transformation towards a more integrated management of gas and electricity networks.

The integration of natural gas and electricity systems has garnered significant interest among researchers [3–5]. These studies offer comprehensive analyses of the operational coordination between gas and electrical systems, emphasizing the critical importance of flexibility. Rubio-Barros [6] explored the planning of joint operations, underscoring the intricate interdependence between natural gas and electricity networks. Additionally, to address supply security in integrated systems, researchers such as [7] have developed simulation models. This research is particularly relevant given the substantial consumption by natural gas thermal generation plants (CGTGNs), which significantly affects overall system gas consumption.

Hibbard et al. [8] provided a comprehensive analysis of the evolving interdependence between natural gas and electricity systems, exploring key influencing factors. Ventosa et al. [9] presented a modeling approach designed to evaluate the technical constraints affecting the operations and availability of natural gas networks. These studies underscore the direct impact on natural gas demand, energy dispatch, and, fundamentally, the reliability and safety of energy systems. Traditionally, research into natural gas and electricity systems has been compartmentalized, reflecting their unique operational

characteristics. Moreover, coordination between natural gas and electricity dispatch has generally been conducted independently, with minimal cross-communication. Despite some studies addressing operational constraints and strategic planning, the integration of gas and electricity markets, along with their models, presents a significant opportunity for further research and development in this critical area.

In Peru, the natural gas (NG) and electricity markets are pursuing initiatives to integrate various energy systems into a unified structure, which is crucial for the overall transformation of the energy sector [10]. This integration is imperative because these systems are interdependent; the risks and uncertainties affecting one system inevitably impact the others. Consequently, it is essential to identify and quantify these risks and develop strategies to mitigate their effects.

Although Peru has taken steps in this direction with the approval of D.S No. 012-2021-EM, which established regulations to optimize the use of natural gas and created the "Natural Gas Manager"—an entity responsible for gathering data on the availability and capacity of NG volumes for short-, medium-, and long-term forecasting—this entity does not have responsibilities for real-time dispatch operations. Therefore, despite these efforts, Peru remains far from achieving the comprehensive integration detailed in [1].

Our objective is to analyze the impact of congestion within the natural gas network on the short-term electricity market within an integrated gas–electric system. We aim to explore the interactions among network parameters, anticipate potential contingency issues in an integrated market, and ensure security and reliability in a competitive market environment.

The main contributions of this research are:

- A comprehensive quantitative and qualitative analysis of the interdependencies between electricity systems and natural gas (NG) networks within an integrated market context. This involves examining how these two energy systems interact and influence each other, identifying key factors that affect their performance and reliability.
- The development and presentation of a reduced equivalent electrical network model for the SEIN (Interconnected Electrical System of Peru) at the 500 kV level. This model simplifies the complex electrical network, making it easier to study and understand. Additionally, an equivalent model for the Peruvian natural gas pipeline system is provided, facilitating a better understanding of the gas network's behavior and its interaction with the electrical system.
- Insights into the economic and physical impacts of congestion in natural gas pipelines on both the short-term electricity market and the transmission network. This includes analyzing how bottlenecks in the gas pipeline system can affect electricity prices, supply reliability, and the overall efficiency of the energy market.
- Proposals for mitigation mechanisms through strategic public policies aimed at alleviating the economic and physical effects of congestion. These mechanisms are designed to ensure the reliable and efficient operation of the integrated gas–electricity system by addressing the root causes of congestion and improving coordination between the gas and electricity sectors.

The structure of this work is as follows: Section 2 presents a model of the integrated gas–electricity market and includes an integrated analysis of the parameters and equations governing both networks. Section 3 provides a detailed examination of the economic and physical impacts resulting from gas network congestion on the short-term market and electrical transmission system. Finally, Section 4 concludes the study by summarizing the key insights and implications derived from the research.

2. The Model Proposed for the Integrated Analysis of the Electricity and Gas Systems

The objective of this research is to evaluate the impact of congestion in the natural gas network on the short-term electricity market dynamics within an integrated gas–electric system. We investigate potential contingencies within this integrated market framework, with a focus on ensuring safety and reliability in a competitive market environment. To achieve this objective, we have refined and extended the models previously developed in [11,12], placing particular emphasis on the interdependencies between the natural gas and electricity markets. Our findings highlight how congestion in natural gas pipelines influences electric power transmission, deepening our understanding of the interconnected operations of these energy systems. This research emphasizes the need for coordinated strategies to maintain system reliability and market competitiveness, making a significant contribution to the body of knowledge on effectively managing interconnected energy systems.

Our research demonstrates the effects of congestion in the natural gas pipeline on electric power transmission networks in short-term operations.

2.1. Gas–Electricity Optimization Model

The planning of wholesale energy markets, often referred to as short-term markets, revolves around economically determining the optimal cost for energy production. This involves a comprehensive consideration of various factors, including minimizing operating costs, dispatching loads from different energy sources, accounting for associated marginal costs, and addressing network constraints [1,13].

A complex interplay of variables and constraints shapes the selection of energy sources and the technologies used for electricity production. These systems are exposed to risks and uncertainties, including the variability of energy sources and the inherent limitations of the technologies employed. Renewable energy plants, in particular, add significant complexity to the planning and operation of energy systems due to their heavy reliance on variable weather conditions. These stochastic elements require sophisticated models and strategies to ensure efficient and reliable energy production under intermittent supply conditions.

In our study, the complex interaction between natural gas sources, the natural gas network, combined-cycle gas turbine generators (CCGTs), and the constraints of transmission network parameters introduces a high degree of interdependence [14]. This interdependence presents significant challenges in calculating optimal dispatch values [15]. Our research focuses on optimizing load dispatch within an integrated gas–electricity system to effectively address these challenges. We utilize a reduced equivalent model at the 500 kV voltage level of the SEIN (National Interconnected Electric System) in Peru, along with an equivalent model for the Peruvian natural gas pipeline. These models, thoroughly detailed by Navarro [11] and Rojas [12], serve as the foundation for our analysis and optimization efforts, aiming to enhance efficiency and reliability in energy dispatch within the integrated system.

2.1.1. Equivalent Reduced Model of the SEIN Peru

The reduced electric model of the SEIN, configured with 12 buses, is characterized by elements represented through their admittances in per unit (p.u.) values. This simplified electrical model of the 12-bus SEIN is designed to make the complex network more manageable for analytical purposes while preserving the crucial characteristics and interactions of the system.

This model simplifies the intricate electrical network into a more tractable form, allowing for detailed study while retaining the essential electrical properties and relationships between the buses. It enables thorough investigations into transmission behaviors, load distributions, and potential bottlenecks. The admittance matrix, as detailed in Table 1, encapsulates the electrical connectivity and characteristics of the buses, providing a quantitative foundation for further analysis and optimization within the integrated gas–electricity framework. This approach facilitates an improved understanding and management of the interconnected energy system.

The outcomes of the power flow analysis conducted on the 12-bus reduced equivalent model of the SEIN Peru at 500 kV are detailed in Table 2.

Table 1. Admittance parameters of the 12-bus reduced equivalent model of the SEIN at 500 kV (in p.u.).

Name Line (500 kV)	From (Bus)	To (Bus)	Admittance Y	PHI (°)	R (p.u.)	X (p.u.)	LIMIT (MVA)
LT La Niña—Trujillo 500 kV	1	2	28.33	−1.49	0.0027	0.0352	420.3
LT Trujillo—Chimbote 500 kV	2	3	62.38	−1.51	0.001	0.016	438.6
LT Chimbote—Carabayllo 500 kV	3	4	23.15	−1.5	0.003	0.0431	376.6
LT Carabayllo—Carapongo 500 kV	4	12	292.1	−1.45	0.0004	0.0034	1379.7
LT Carapongo—ChilcaCTM 500 kV	12	6	129.34	−1.48	0.0007	0.0077	780
LT Chilca—Poroma 500 kV	6	5	20.99	−1.49	0.0037	0.0475	646.3
LT Poroma—Ocoña 500 kV	5	9	71.51	−1.37	0.0028	0.0137	491
LT Ocoña—San José 500 kV	9	8	140.08	−1.37	0.0014	0.007	267.5
LT San José—Montalvo 500 kV	8	7	166.09	−1.37	0.0012	0.0059	0
LT Montalvo—Yarabamba 500 kV	7	11	76.16	−1.5	0.0009	0.0131	584.2
LT Yarabamba—Poroma 500 kV	11	5	35.48	−1.43	0.004	0.0279	0
LT Poroma—Colcabamba 500 kV	5	10	47.42	−1.44	0.0028	0.0209	889.2

Table 2. Load flow analysis results for the 12-bus reduced equivalent model of the SEIN Peru at 500 kV.

Number Bus	Name Bus	Voltage p.u.	Angle (°)	Load MW	Load MVAR	Gen MW	Gen MVAR	Base kV
B1	La Nina 500 kV	1.000	−40.16	420.3	230	96.3	32.7	500
B2	Trujillo 500 kV	1.000	−33.54	438.6	224.7	30.3	39.5	500
B3	Chimbote 500 kV	1.000	−26.73	376.6	87.1	333.5	167.8	500
B4	Carabayllo 500 kV	1.000	−6.63	1379.7	900.5	908.6	643.6	500
B5	Poroma 500 kV	0.969	−7.39	780	101.7	0	0	500
B6	Chilca 500 kV	1.000	0	646.3	517.3	1841	735.5	500
B7	Montalvo 500 kV	1.000	−10.49	491	268.6	167	150.7	500
B8	San Jose 500 kV	0.999	−10.67	267.5	70.5	0	316	500
B9	Ocoña 500 kV	0.986	−9.60	0	−96.8	0	0	500
B10	Colcabamba 500 kV	1.000	−1.74	584.2	452.5	1332.6	307.6	500
B11	Yarabamba 500 kV	1.000	−7.64	0	−150	383	167	500
B12	Carapongo 500 kV	1.000	−4.11	889.2	646.8	1251.3	−1.3	500

Figure 1 depicts the 12-bus reduced equivalent model of the SEIN at the 500 kV voltage level.

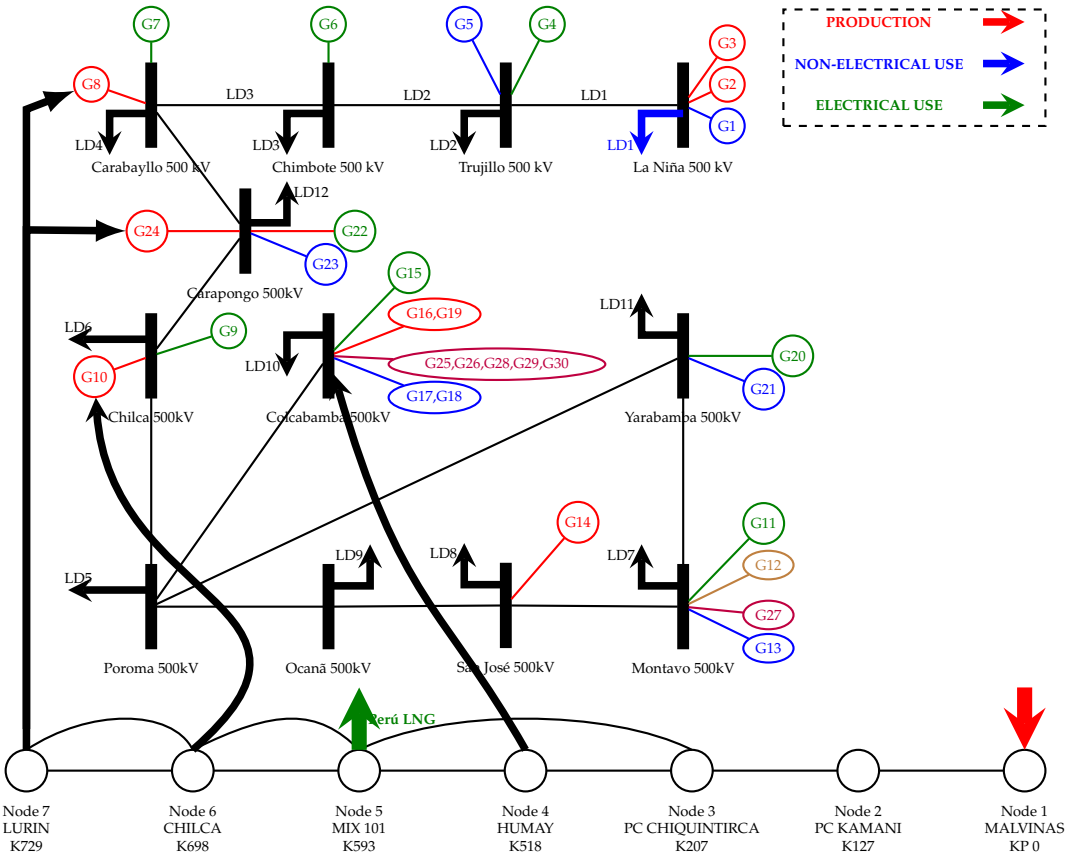

Figure 1. Interaction diagram of the Peruvian integrated gas–electricity system.

2.1.2. Equivalent Model of the Peruvian Natural Gas Pipeline Network

The equivalent model of the natural gas (NG) pipeline network is designed to conform to the parameters and constraints governing the relationships between gas flows and pressures. Addressing the challenge presented by the non-linear nature of these flow-pressure relationships, we have developed a linear approximation [16]. This approximation is based on an equivalent model of the NG network that incorporates all relevant network parameters, facilitating an accurate representation of these critical interactions.

Table 3 displays the lengths of the main natural gas pipeline sections, organized according to their pipe diameters. This table includes segments owned by various operators, such as Peru LNG and the Loop Coast, offering a comprehensive overview of the network's physical structure.

Table 3. Main parameters of the equivalent model of the Peruvian gas pipeline network (adapted from Osinergmin).

Line	Node Start	Node End	Has Compresor	Diameter (Inch)	Length km	Accountability
1	Node 1 (Malvinas)	Node 2 (Kamani)	YES	32	126.7	main network
2	Node 2 (Kamani)	Node 3 (Chiquintirca)	YES	32	81.27	main network
3	Node 3 (Chiquintirca)	Node 4 (Humay)	NO	24	309.93	main network
4	Node 4 (Humay)	Node 5 (Mix 101)	NO	18	75.24	main network
5	Node 3 (Chiquintirca)	Node 5 (Mix 101)	NO	34	406	Peru LNG
6	Node 5 (Mix 101)	Node 6 (Chilca)	NO	18	105	main network
7	Node 5 (Mix 101)	Node 6 (Chilca)	NO	24	105	Loop coast
8	Node 6 (Chilca)	Node 7 (Lurín)	NO	18	31.16	main network
9	Node 6 (Chilca)	Node 7 (Lurín)	NO	24	31.16	Loop coast

Table 4 provides the URL coordinates for the nodes, while Table 5 presents the maximum and minimum natural gas flows, taking into account both electrical and non-electrical demands.

Table 4. URL coordinates of the nodes of the Peruvian gas pipeline network (Adapted from https://observatorio.osinergmin.gob.pe/ accessed on 15 March 2023).

Node	Name	KP	Zone	North	East
1.	Malvinas	KP 0	18	8,689,907.55	724,013.26
2.	Kamani	KP 127	18	8,599,403.00	691,070.00
3.	Chiquintirca	KP 207	18	8,599,333.00	691,017.00
4.	Humay	KP 517.9	18	8,480,890.00	404,048.00
5.	Mix 101 (CUA)	KP 594.9	18	8,536,618.00	361,063.00
6.	Chilca	KP 699	18	8,614,339.00	314,286.00
7.	Lurin	KP 729	18	8,640,336.00	300,970.00

Table 5. Maximum and minimum volumes, considering electrical and non-electrical demands (adapted from Osinergmin).

Node	Name	Level Producción		Use Max (Elect/No Elect)		Level of Pressure	
		Min	Max			Min (bar)	Max (bar)
		MMPCD	MMPCD	MMPCD	MMPCD		
1.	MALVINAS	460	1605	0	0	147	147
2.	KAMANI	460	1605	0	0	136	147
3.	CHIQUINTIRCA	225	435	0	0	109	147
4.	HUMAY	196	386	49	0	120	135
5.	MIX 101	416	936	0	620	113	102
6.	CHILCA	203	516	420	0	104	54
7.	LURIN	203	516	0	516	104	46

Figure 1 showcases the integration of the 12-bus reduced equivalent model of the SEIN with the equivalent model of the Peruvian natural gas pipeline network.

2.2. Objetive Function

Building on the foundational research presented in [11,12], this paper extends its models to delve deeper into the complex interdependencies between the natural gas and electricity markets. We have developed an optimization function specifically tailored for the competitive dynamics of an integrated gas–electricity market. The primary objective of this optimization is to maximize social profit, which effectively translates into minimizing the overall social costs associated with energy provision. This includes reducing the production costs of electricity, decreasing expenditures on natural gas supplies, and lowering the operational costs of the natural gas network. Through this framework, our goal is to enhance the cost-effectiveness and efficiency of the energy supply system, thereby delivering economic and societal benefits.

The optimization model introduced in this study features the role of a gas–electricity system operator, who is tasked with the real-time management of both the electrical grid and the natural gas pipeline network. The fundamental aim of this model is to guide the operator in minimizing costs by carefully balancing operating expenses, pipeline transportation costs, and fuel costs for natural gas-fired power plants. This comprehensive approach to cost management emphasizes the operator's critical role in optimizing the efficiency and economic performance of the integrated system.

To support the effective implementation and analysis of this model, we establish the following assumptions:

- Power Balance: There must be a continuous balance between energy supply and demand, ensuring that load flows are within network restrictions.

- Individual Generator Constraints: Each generator operates under specific constraints, including dispatch price, generation limits, and other operational limitations.
- Power Transmission Constraints: The transmission system is governed by constraints to ensure its reliable and secure operation. These include line capacities, voltage limits, and other transmission-related factors.
- Natural Gas Source and Pipeline Limits: The model considers limitations on the availability of natural gas and the capacity of pipelines, ensuring that the supply remains within specified limits.
- Natural Gas Network Constraints: The natural gas network faces operational constraints, such as pressure limits, flow capacity limits, and other network-related constraints.
- Coupling Constraints: There are specific constraints on the coupling between the electrical and gas systems, ensuring coordinated operation while respecting the operational limits and capabilities of each system.
- Hydroelectric Power Plants: The model assumes a linear cost function for hydroelectric power plants, which simplifies representation and excludes a hydro-thermal coupling.
- Time Resolution: The model uses a one-hour time resolution to analyze a 24-h day, allowing it to capture temporal dynamics and variations in demand and generation profiles.
- Transmission Costs: The objective function of the model excludes transmission costs, focusing primarily on minimizing generation and natural-gas-related costs.

These assumptions and constraints shape the formulation and analysis of the optimization model within the integrated gas–electricity market framework.

$$FO = EC + GC + TC \tag{1}$$

$$EC = \sum_{g=1}^{Gen} \sum_{t=1}^{24} (b_g * P_g^2(t) + a_g * P_g(t) + c_g + C_{Diesel} + C_{rer} + C_{res}) \tag{2}$$

$$GC = \sum_{n=1}^{NGs} \sum_{t=1}^{24} (S_n(t) * \ p_{ng}) \tag{3}$$

$$TC = \sum_{l=1}^{PG} \sum_{t=1}^{24} (f_{nm}(t) * p_{tg}) \tag{4}$$

where:

$P_g(t)$: Active Power delivered by generator g at period t, measured in [MW].
a_g, b_g, *and* c_g: Characteristic constants for each gas and diesel thermal generator, used in the quadratic equation for computing the cost of energy production from each bus generator. These constants depend on the power output of the generator and are measured in [USD/MW^2], [USD/MW], and [USD], respectively.
C_{Diesel}: Cost of Generation with Diesel in [USD].
C_{rer}: Cost of generation with conventional and non-conventional renewable sources in [USD].
C_{res}: Cost of energy storage system in [USD] that remains fixed throughout the period.
S_n: NG supply at node n in period t, measured in [10^6 m^3/h].
P_{ng}: Unit price of NG, measured in [USD/m^3].
$f_{mn}(t)$: NG flow from node m to node n in period t, measured in [10^6 m^3/h].
p_{tg}: Unit cost of NG transportation in [USD/m^3].
PG: number of pipes in the gas network.
NGs: Number of supply points in the NG network.
Gen: Number of power plants in the network.

2.2.1. Electrical System

For a typical bus "i", the power flow equations can be articulated by considering the network's impedance and the potential difference between buses "i" and "j", expressed in polar coordinates. These fundamental equations encompass both components of power: the active power, denoted as P_i, and the reactive power, represented by Q_i. Specifically, the equations can be expressed as follows:

(a) Power flow:

$$P_i = \sum_{j=1}^{N} \left|Y_{ij} V_i V_j\right| \cos\left(\theta_{ij} + \delta_j - \delta_i\right) \qquad \forall\, t \tag{5}$$

$$Q_i = -\sum_{j=1}^{N} \left|Y_{ij} V_i V_j\right| \sin\left(\theta_{ij} + \delta_j - \delta_i\right) \qquad \forall\, t \tag{6}$$

Notation:

$$Y_{ij} = \left|Y_{ij}\right|\langle\theta_{ij} = \left|Y_{ij}\right| \cos\theta_{ij} + j\left|Y_{ij}\right| \sin\theta_{ij} = G_{ij} + jB_{ij} \tag{7}$$

$$V_i = |V_i|\langle\delta_i = |V_i|(\cos\delta_i + j\sin\delta_i) \tag{8}$$

$$-P_{km}^{max} \leq P_{km} \leq P_{km}^{max} \tag{9}$$

where:
P_i: Active power at bus i during period t, measured in megawatts (MW);
Q_i: Reactive power generated at bus i during period t, measured in megavolt-amperes reactive (MVAR);
Y_{ij}: Impedance of the line between bus i and j, incorporating both resistance and reactance components;
θ_{ij}: Angle of total line admittance between bus i and j, representing the phase difference that affects power flow;
δ_i: Voltage phase shift angle at bus i, indicating the difference in phase angle of the voltage relative to a reference point;
P_{km}^{max}: Maximum limit of active power transferable in the section from node k to node m, specified in megawatts (MW);
P_{km}: Active power in the section from bus k to bus m, measured in megawatts (MW);

(b) Losses in the electrical network:

$$P_L = \sum_{i=1}^{N} P_{gi,t} - \sum_{i=1}^{N} P_{di,t} \qquad \forall\, t \tag{10}$$

$$Q_L = \sum_{i=1}^{N} Q_{gi,t} - \sum_{i=1}^{N} Q_{di,t} \qquad \forall\, t \tag{11}$$

where:
P_L: Active power losses within the network during period t, measured in megawatts (MW);
Q_L: Reactive power losses within the network during period t, measured in megavolt-amperes reactive (MVAR);
$\sum_{i=1}^{N} P_{gi,t}$: Total active power delivered by the generators in the network during period t, aggregated across all N buses, in MW;
$\sum_{i=1}^{N} P_{di,t}$: Total active power demand at all N buses in the network during period t, in MW;
$\sum_{i=1}^{N} Q_{gi,t}$: Total reactive power supplied by the generators in the network during period t, aggregated across all N buses, in MVAR;
$\sum_{i=1}^{N} Q_{di,t}$: Total reactive power demand at all N buses in the network during period t, in MVAR;
N: The total number of buses in the electrical network.

(c) Power balance:

$$\sum_{g=1}^{G} P_{gi,t} - P_{di,t} = \sum_{j=1}^{N} \left|Y_{ij} V_{i,t} V_{j,t}\right| \cos\left(\theta_{ij} + \delta_{j,t} - \delta_{i,t}\right) \qquad \forall\ i,\ t \tag{12}$$

$$\sum_{g=1}^{G} Q_{gi,t} - Q_{di,t} = -\sum_{j=1}^{N} \left|Y_{ij} V_{i,t} V_{j,t}\right| \sin\left(\theta_{ij} + \delta_{j,t} - \delta_{i,t}\right) \qquad \forall\ i,\ t \tag{13}$$

$$V_{min} \leq\ V_{i,t} \leq\ V_{max}\ \ldots\ \forall\ i,\ t \tag{14}$$

$$\delta_{min} \leq\ \delta_{i,t} \leq\ \delta_{max} \ldots\ \forall i,\ t \tag{15}$$

where:
$\sum_{g=1}^{G} P_{gi,t}$: Total variable active power delivered by generator g to bus i at time t, measured in megawatts (MW);
$\sum_{g=1}^{G} Q_{gi,t}$: Total variable reactive power delivered by generator g to bus i at time t, measured in megavolt-amperes reactive (MVar);
$P_{di,t}$: Total active power load on bus i during period t, measured in MW;
$Q_{di,t}$: Total reactive power load on bus i during period t, measured in MVar;
The units of measurement for these variables are specified as follows: active power is expressed in megawatts (MW) and reactive power in megavolt-amperes reactive (MVar), aligning with the standard units of power in electrical engineering.
The units are in values per unit (p.u.), the units of active power are in MW, and the units of reactive power are in MVar.

2.2.2. Natural Gas Network

(a) Energy Dispatch Equations for Thermal Power Plants Fueled with Natural Gas (NGFTPUs):
Taking into account a pipeline network composed of various nodes, each with a defined requirement for natural gas (NG) aimed at generating electricity, the formulas documented in [17] serve to characterize the operation of each Natural Gas Fueled Thermal Power Unit ($NGFTPUs$).

$$P_{gi,min} \leq\ P_{gi,t} \leq P_{gi,max} \ldots \forall i,\ t \tag{16}$$

$$\sum_{n=1}^{NGs} P_{gi}(e_n) = P_{di} \ldots\ \ \forall\ t \tag{17}$$

$$P_{gi} = \eta(e_n) * \ LHV * \ e_n \tag{18}$$

where:
P_{gi}: Power generated in MW by NG thermal plant;
e_n: Flow of NG from node n to the generator, measured in cubic meters per second (m^3/s);
η: Efficiency of the thermal power plant, a dimensionless coefficient;
LHV: Low Heating Value Constant equivalent to 35.07 MW/(m^3/s) .
Equation (16) delineates the capacity constraints for the Natural Gas Fueled Thermal Power Units (NGFTPUs) situated at node n within the pipeline network. It is essential to highlight that NGFTPUs operate with a minimum non-zero capacity to maintain operational stability. This requirement is crucial for ensuring the reliable and secure operation of the NGFTPUs.
Equation (17) specifies the electrical power demand P_{gi}, highlighting the system's reliance on thermal generation using natural gas. It demonstrates how Natural Gas Fueled Thermal Power Units (NGFTPUs) dynamically manage energy dispatch in response to system demand, contingent upon the natural gas network's capacity to meet gas requirements. The aim is to optimize operation efficiency, thereby reducing both energy production and gas transportation costs within the pipeline network.

Equation (18) quantifies the relationship between the input of NG fuel and the resulting production of electrical energy, reflecting the efficiency and operational characteristics of the combined-cycle NGFTPUs.

Equation (16) outlines the generation capacity constraints of the Natural Gas Fueled Thermal Power Units (NGFTPUs) at node n. It is critical to recognize that the correlation between energy generation and the flow of natural gas is complex and non-linear, influenced by a multitude of factors. These encompass the specific attributes of the thermal power plant, the inherent properties of the natural gas, and environmental variables pertinent to the location, such as altitude (measured in meters above sea level) and climatic conditions (including temperature and relative humidity). As documented in [17], this intricate interplay means that energy output in a combined cycle plant is best represented through a cubic function of natural gas flow. Thus, this nuanced relationship can be encapsulated in the subsequent mathematical expression.

$$P_{gi}(e_n) = k_3 e_n^3 + \ k_2 e_n^2 + k_1 e_n \tag{19}$$

In Equation (19), the coefficients k_3, k_2, and k_1 depend on the specific characteristics of the natural gas thermal generation plants. However, determining these coefficients can be a complex task. As a result, for the purposes of the research work conducted in [17,18], a simplified approximation was employed. The simplified Equation (19) was applied to the test networks in the research work, assuming that for each unit of power produced in megawatts (MW), approximately 0.05 m^3/s or 4320 m^3/day of natural gas is required.

$$P_{gi}(e_n) = k_1 * \ e_n \tag{20}$$

where:

k_1 = 0.0023148 MWatts·day/106 m^3

(b) NG flow equations:

As discussed in Section 2.1.2, we established that the pipeline network's equivalent model consists of nodes for importing or exporting natural gas (*NG*), adhering to the principle of mass balance at each node. Consequently, the *NG* injection flows into a node are balanced by the *NG* flows allocated for both electrical generation and non-electrical uses, as supported by the findings in [17].

$$S_n + \sum_m f_{mn} = \sum_j f_{no} + d_n + e_n \qquad \forall\, t \tag{21}$$

where:

S_n: NG supply at node n, measured in cubic meters per hour (m^3/h) or cubic meters per day (m^3/day);

f_{mn}: NG flow from node m to node n, expressed in cubic meters per hour (m^3/h) or cubic meters per day (m^3/day);

e_n: NG flow from node n to the generator, measured in cubic meters per second (m^3/s);

d_n: NG demand for non-electric use at node n, specified in cubic meters per hour (m^3/h) or cubic meters per day (m^3/day).

Equation (21) shows the natural gas flow balance at node "n". Likewise, it is important to consider that these flows are influenced by various characteristics associated with natural gas, including the natural gas pressure at the inlet and outlet of the node, as well as the pipe section. To describe the relationship between pressure and natural gas flow, the Weymouth Equation (22) is employed. This equation defines the relationship between pressures and the flow of NG, providing

a valuable tool for analyzing and understanding the behavior of natural gas flow within the system.

$$Sign(f_{nm}){f_{nm}}^2 = {C_{nm}}^2(p_n^2 - p_m^2) \qquad \forall\, t \tag{22}$$

$${f_{nm}}^2 \leq -{C_{nm}}^2(p_n^2 - p_m^2) \qquad \forall\, t \tag{23}$$

$$p_{n,min} \leq\ p_n \leq\ p_{n,max} \qquad \forall\, t \tag{24}$$

$$f_{nm,min} \leq\ f_n \leq\ f_{nm,max} \qquad \forall\, t \tag{25}$$

$$S_{n,min} \leq S_n \leq S_{n,max} \qquad \forall t \tag{26}$$

where:
p_n: Pressure at node n, measured in bars;
p_m: Pressure at node m, in bars;
C_{nm}^2: Constant reflecting the chemical composition of the NG and the characteristics of the nm section of the NG pipeline, given in cubic meters to the sixth power per square bars ($m^6/bars^2$).
Subject to the following constraints:
$f_{nm,max}$: Maximum NG flow from node n to node m, specified in cubic meters per hour (m^3/h);
$f_{nm,min}$: Minimum NG flow from node n to node m, in cubic meters per hour (m^3/h);
$p_{n,max}$: Maximum pressure allowed at node n, measured in bars;
$p_{n,min}$: Minimum pressure allowed at node n, in bars;
$S_{n,max}$: Maximum limit of the NG supply delivered by the producer or importer node n (m^3/h);
$S_{n,min}$: Minimum limit of the NG supply delivered by the producer or importer node n (m^3/h)
The constant C_{nm} depends on the characteristics of the NG pipeline, such as the diameter, length, and roughness of its walls, among other aspects, and the chemical composition of the NG.
The constant C_{nm} is influenced by several factors related to the natural gas (NG) pipeline, including its diameter, length, the roughness of its internal walls, among other physical characteristics, as well as the chemical composition of the NG itself. If $f_{nm} > 0$, this indicates that the natural gas (NG) flow is directed from node n to node m. Conversely, if $f_{nm} < 0$, it signifies that the NG flow reverses, moving from node m to node n. Equation (23) models the NG flow within the pipeline network as a quadratic function of the pressure at the respective end nodes. Specifically, when the inlet pressure at node n exceeds the outlet pressure at node m ($p_n > p_m$), it results in natural gas flowing from node n to node m ($f_{nm} > 0$).
Equation (23) imposes a unique constraint at each node, often necessitating the use of compressors. These devices are crucial for boosting the pressure at specific nodes where an increase in natural gas (NG) pressure is required. By enhancing the pressure, compressors enable a greater flow of NG than what would be possible under standard conditions, thereby aiding in the efficient redirection of NG throughout the network. For instance, in scenarios like in Peru, elevating the NG pressure is essential for transporting gas across challenging terrains such as the Andes mountains. Consequently, compressors allow for bypassing the maximum flow constraints, facilitating the injection of larger volumes of NG into the gas pipeline transmission networks. Nonetheless, it remains critical to ensure that pressure levels are kept within their prescribed limits to preserve the operational integrity and safety of the system.
Similarly, constraint (26) regarding the supply of natural gas S_n adapts dynamically. If $S_n > 0$ at node n, it signifies that the node acts as a producer or importer of natural gas. On the other hand, if $S_n < 0$ at node n, it denotes that the node serves as a consumer of natural gas, encompassing both electrical and non-electrical

consumption. This constraint effectively captures the varied roles and functions of nodes within the natural gas network, accounting for the intricate balance of supply and demand.

The function $Sign(f)$, introduced in Equation (22), is utilized to determine the direction of natural gas (NG) flow.

$$Sign(x) = \begin{cases} 0, & if\ x = 0 \\ 1, & if\ x > 0 \\ -1, & if\ x < 0 \end{cases} \tag{27}$$

For instance, if the flow from node m to node n is designated as positive, and the outcome of the simulation yields $f_{mn} > 0$, this indicates that the natural gas (NG) flow direction is indeed from node m to node n. Conversely, should the simulation result in $f_{mn} < 0$, it implies that the NG flows in the pipeline are directed from node n to node m.

The inequality presented in Equation (25) highlights the physical constraints inherent to gas pipelines, specifically addressing the maximum and minimum flow limits of natural gas (NG) that delineate flow directionality within the system. Under typical circumstances, the lower limit is set to zero, indicating no reverse flow is allowed. However, in the presence of compressors within the pipeline, a minimum flow rate greater than zero may be established to ensure effective gas transportation. Conversely, the maximum flow rate is determined by the pipeline's capacity and can be quantified through the subsequent equation:

$$f_{nm} = \sqrt{C_{nm}^2 (p_n^2 - p_m^2)} \tag{28}$$

If $f_{nm} > 0$, it indicates that the natural gas (NG) flow is directed from node i to node j. Conversely, if $f_{nm} < 0$, the NG flow reverses, moving from node j to node i. To accurately model this behavior, a binary variable is incorporated into the equation, transforming the formulation into a combinatorial problem.

The variable C_{nm}, featured in Equations (29) and (30), is defined as follows:

$$C_{nm} = 96.074830 * 10^{-15} \frac{D_{nm}^5}{\lambda_{nm} * z * T * L_{nm} \delta} \tag{29}$$

$$\frac{1}{\lambda_{nm}} = 9 \left[2\ log\ \left(\frac{3.7\ D_{nm}}{\varepsilon} \right) \right]^2 \tag{30}$$

where:

D^{nm}: Internal diameter of the natural gas (NG) duct, measured in millimeters (mm);

z: NG compressibility factor, a dimensionless unit valued at 0.8;

T: Constant temperature for NG, set at 281.15 Kelvin (K);

Lnm: Length of the NG pipeline section from node n to node m, in kilometers (km);

δ: Density of NG relative to air, a dimensionless value of 0.6106 and;

ε: Absolute roughness of the NG duct, quantified as 0.05 mm.

3. Case Study and Results Analysis

The set of equations described above defines a mixed non-linear optimization problem. This is primarily due to the presence of binary terms, non-linear relationships, and the constraints associated with both the gas pipeline system and the thermoelectric generation system included in the proposed model, as illustrated in Figure 1. The combination of these elements results in a complex optimization problem that requires specialized techniques and algorithms to obtain optimal solutions. The integrated model encompasses the interdependencies between the gas pipeline system and the thermoelectric generation system, enabling a comprehensive analysis and optimization of the integrated energy system.

To simplify practical considerations, it was determined necessary to group the 182 generation plants in the system into 24 plants with distinct technologies but similar operating costs. This grouping helps streamline the analysis and management of the system, as it reduces the complexity associated with individual plant-level considerations. By categorizing the plants based on their technology and comparable operating costs, it becomes more feasible to implement effective optimization strategies and make informed decisions regarding the operation and planning of the integrated energy system.

To assess the impact of congestion on the natural gas network, it was necessary to deliberately impose constraints on the pipeline's capacity. By simulating congestion and analyzing the network's behavior, the effects on bus prices and the resulting low energy production costs can be studied. This analysis considers the demand of a typical day, as indicated in Table 6. By examining this scenario, a comprehensive understanding of the system's response to congestion and its implications on energy production costs can be obtained.

Table 6. Electrical demand SEIN (GW) adapted from Coes.

Hour	16 August 2022	Hour	16 August 2022	Hour	16 August 2022
01:00	5.99	09:00	6.61	17:00	6.97
02:00	5.87	10:00	6.87	18:00	6.80
03:00	5.75	11:00	6.99	19:00	7.06
04:00	5.76	12:00	7.11	20:00	7.09
05:00	5.83	13:00	6.94	21:00	7.05
06:00	5.96	14:00	6.90	22:00	6.92
07:00	6.19	15:00	7.01	23:00	6.66
08:00	6.35	16:00	7.06	00:00	6.29

3.1. Congestion Effects of a Natural Gas Pipeline

To analyze the behavior of the integrated gas–electricity system under congestion scenarios, it is important to recognize that operational congestion events are often not prevalent under typical real-world conditions, as noted in [11]. To simulate and study these hypothetical conditions, we deliberately reduce the maximum capacity of the primary natural gas pipeline within the system. By imposing this constraint, we can effectively induce congestion scenarios for a typical demand profile corresponding to the year 2022. These capacity reductions could result from failures or scheduled maintenance.

To explore a range of congestion levels, we progressively reduce the maximum capacity of the natural gas transmission network by varying percentages, starting from a 10% reduction. The reduction continues until reaching a percentage where the results no longer converge or remain stable. This approach enables us to observe the system's response under different levels of congestion and evaluate its impact on the integrated gas–electricity system.

The simulation outcomes, depicted in Figure 2, elucidate the impact of reducing the main pipeline's maximum capacity on the electricity production costs within the integrated system. Initially, when the pipeline capacity is diminished to 50% of its original size, the production costs remain unaffected. However, further reductions to 60% and 70% lead to a noticeable increase in production costs. This pattern reveals that the system possesses a certain resilience to reductions in pipeline capacity without incurring additional costs. Yet, surpassing a critical threshold, estimated between a 60% to 70% reduction, congestion-induced constraints begin to adversely affect the system's efficiency and the cost-effectiveness of electricity production. These results highlight the critical need for maintaining an optimal balance between pipeline capacity and electricity production costs to ensure the efficient functioning of the integrated gas–electricity network.

Figure 2 illustrates the cost implications for electricity production as a function of reducing the maximum capacity of the main natural gas pipeline.

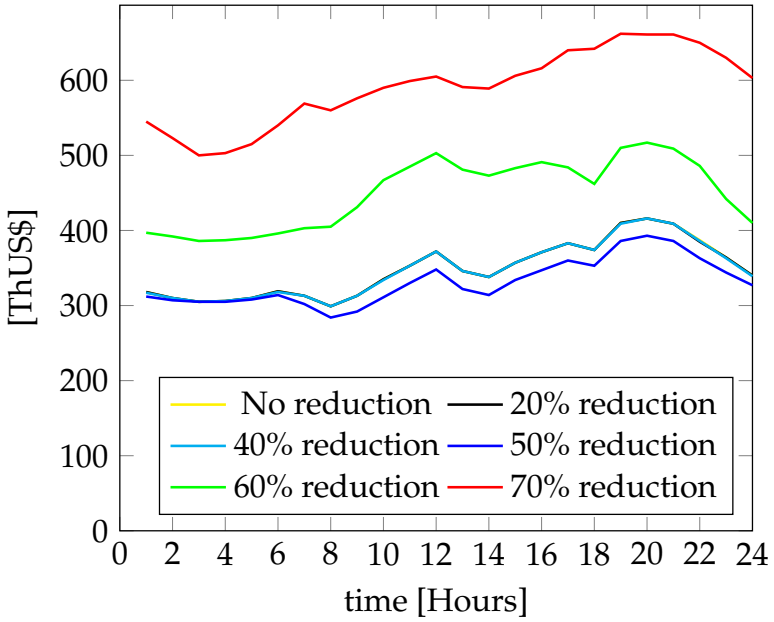

Figure 2. Cost of electricity production considering reduction of the maximum capacity of the main NG pipeline.

Figure 3 depicts the relationship between the costs of natural gas consumption and the demand for electricity generation under congestion scenarios. It reveals an inverse correlation between the cost of electricity production and the costs associated with natural gas consumption. Notably, as the maximum capacity of the main natural gas pipeline is curtailed by over 50%, we observe a decrease in the costs of natural gas for electricity generation. Moreover, a reduction surpassing 70% leads to a scenario where the costs associated with natural gas consumption effectively drop to zero. This illustrates the complex dynamics between pipeline capacity limitations and the economic aspects of energy production within the system.

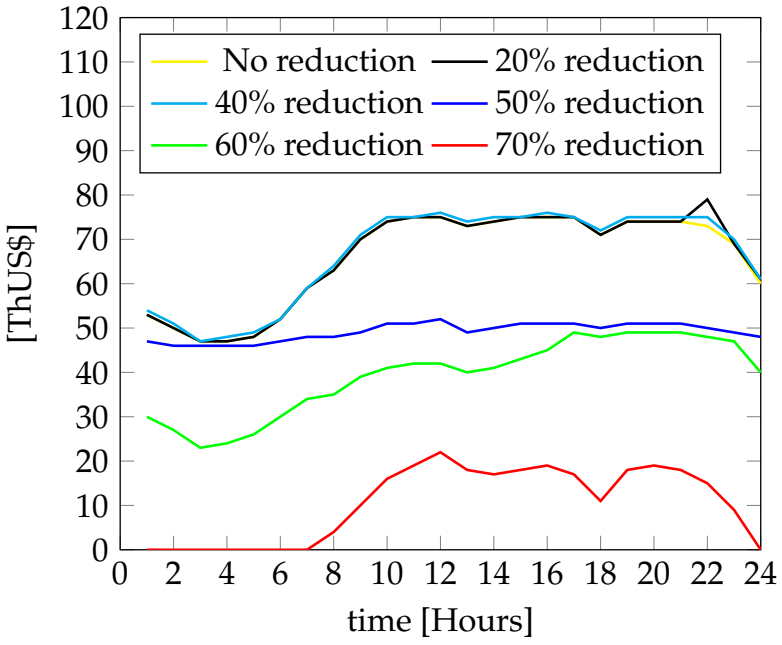

Figure 3. Natural gas consumption costs to cover electricity demand with reduction of the maximum capacity of the main natural gas pipeline.

Figures 2 and 3 provide a comprehensive view of the energy production costs within the integrated gas–electricity system, under scenarios of varying reductions in the maximum capacity of the main natural gas pipeline. The analyses reveal that production costs within the system begin to escalate once the pipeline capacity reduction surpasses 50%. This increase in costs can be attributed to a multitude of factors, such as the necessity to resort to generation plants with higher marginal costs, the lack of contribution from hydroelectric generation plants, and the constrained availability of natural gas, which limits the operational capacity of NG-fueled plants to meet the existing demand. These insights underscore the critical interdependencies between pipeline capacity and the operational economics of the integrated energy system.

Based on the comprehensive analysis of congestion effects within the natural gas pipeline network, and taking into account the implications of reducing the main natural gas pipeline's maximum capacity, significant disparities have been identified under specific conditions across two predefined scenarios (Scenario 1 and Scenario 2). These conditions highlight the differential impact of pipeline capacity constraints on the system's efficiency and cost-effectiveness, underscoring the nuanced dynamics that characterize each scenario's unique challenges and opportunities.

Conditions
No reduction in the capacity of the NG pipeline
Reduction of the capacity of the NG pipeline to 60%
Reduction of the capacity of the NG pipeline to 70%

Hence, we will now discuss the effects on the behavior of the plants, the effects on the bus prices, and the effects on the load flows in these three conditions for each scenario.

3.2. Impact of Reduced NG Pipeline Capacity on Generation Plant Operations

The operational dynamics of generation plants, particularly hydroelectric plants, undergo significant changes as the capacity of the main natural gas (NG) pipeline is reduced beyond a 50% threshold. Under such conditions, hydroelectric plants are called upon to increase their dispatch to meet the persistent demand for electricity. Nonetheless, their capacity to compensate for the reduced NG supply is bounded by their maximum operational volumes and the limitations posed by the capacities of the transmission lines to which they are connected. Figure 4 delineates the operational behavior of hydroelectric plants within these constraints, providing insight into how transmission line capacities further influence their ability to respond to demand.

The analysis of both scenarios reveals a consistent pattern: there is a notable dispatch overlap for hydroelectric plants between situations where there is no reduction in NG pipeline capacity and scenarios with a 60% reduction. This observation underscores the resilience of hydroelectric plants in contributing towards electricity demand satisfaction, even amid substantial reductions in the availability of natural gas. Such findings highlight the critical role of hydroelectric plants in maintaining system stability and mitigating the impacts of NG supply constraints.

It is reasonable to anticipate that with a lower supply of natural gas, resulting from the reduction in the maximum capacity of the main natural gas pipeline, the demand must be met by plants with higher operating costs, such as Diesel plants. These plants quickly increase their dispatch, leading to higher energy production costs, as illustrated in Figure 4.

Conversely, natural gas thermal generation decreases due to the effect of reducing the maximum capacity of the natural gas main pipeline. Notably, as congestion intensifies and reaches the 70% threshold, dispatch tends to reach zero.

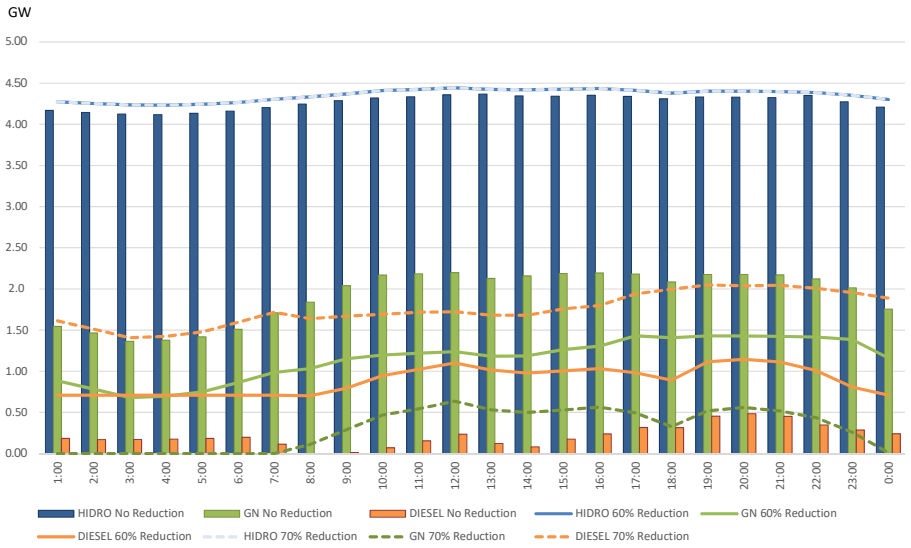

Figure 4. Behavior by kind of electricity generation considering the reduction of the maximum capacity of the main natural gas pipeline.

3.3. Variation of Bus Prices in Scenarios Considering the Reduction of the Maximum Capacity of the Main Natural Gas Pipeline

As the reduction in the maximum capacity of the natural gas pipeline increases, generation through natural gas thermal plants decreases, resulting in an increase in bus prices. While some bus prices, like those of bus 4, exhibit minimal variations, there are cases where significant bus price fluctuations are observed.

For instance, in Figure 5, bus 6 displays a trend where, as the reduction in the maximum capacity of the main natural gas pipeline increases, the bus price approaches its limit of 50 USD/MW.

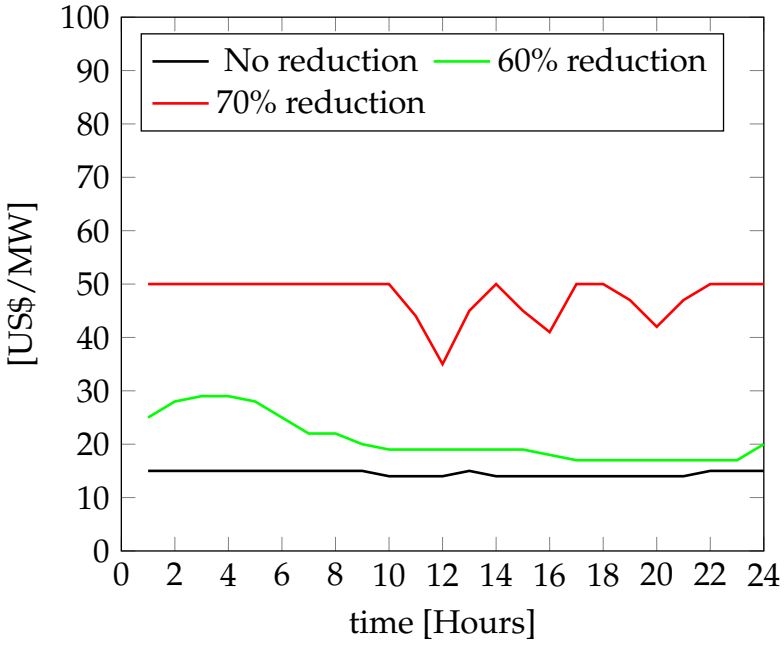

Figure 5. Variation of the price in bus 6 considering the reduction of the maximum capacity of the main natural gas pipeline.

In the case of bus 12, as depicted in Figure 6, it is evident that as congestion intensifies, the price on the bus approaches its upper limit of 80 USD/MW.

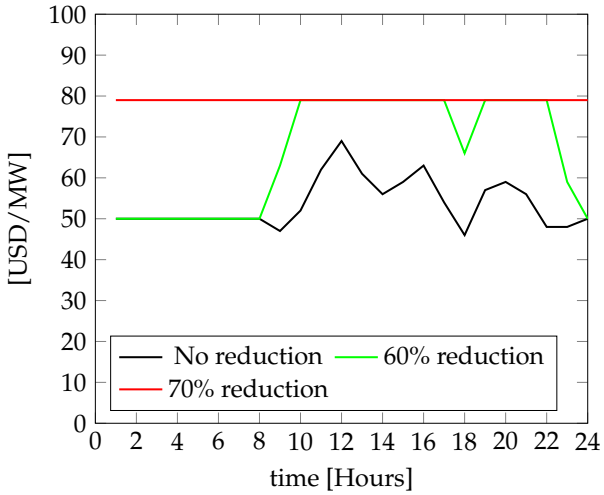

Figure 6. Variation of the price in bus 12 considering the reduction of the maximum capacity of the main natural gas pipeline.

3.4. Effects on Load Flows in Congestion Scenarios of a Natural Gas Pipeline

The energy flows between various buses exhibit distinct behavior when the reduction of the maximum capacity of the main natural gas pipeline approaches approximately 70% of its total capacity. At this juncture, the flows tend to reverse their direction or, in the absence of reversal, saturate the transmission network.

This behavior aligns with expectations, as the model's objective is to optimize production costs while adhering to network constraints and achieving an optimal dispatch strategy.

Load flows display notable variability in response to even minor demand signals, leading to significant fluctuations in power flows between bus 12 and 4. This dynamic response is visible in Figure 7, illustrating load flows between bus 12 and 4 under varying demand scenarios. These fluctuations underscore the system's sensitivity to even slight changes in load requirements.

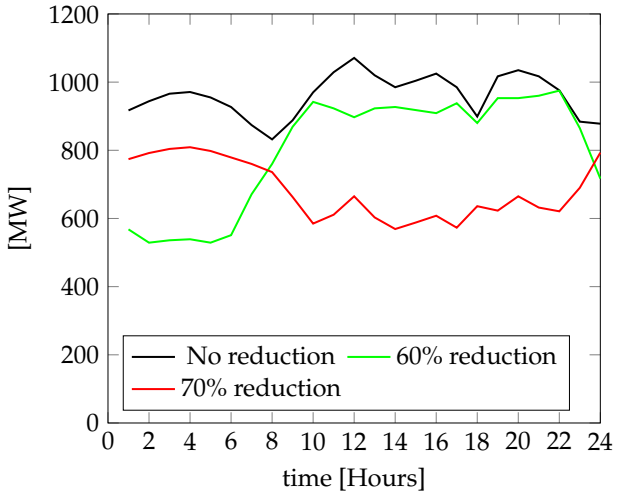

Figure 7. Load flow changes from bus 12 to 4 with reductions in the main natural gas pipeline's capacity

The dynamics of power flows from bus 6 to bus 12, as depicted in Figure 8, highlight the impact of natural gas pipeline capacity on the electrical grid. When the main natural gas pipeline operates at full capacity, the line between bus 6 and 12 typically reaches its maximum load limit. However, with increasing reductions in the pipeline's capacity, there is a noticeable decline in the flow through this line. This trend is directly linked to the diminishing natural gas supply, which, in turn, affects the power generation and subsequent

flows between these buses. Thus, while unrestricted pipeline capacity allows for optimal line utilization, any constraints on the natural gas supply lead to a proportional decrease in power flows, illustrating the tight interconnection between natural gas availability and electrical grid performance.

Figure 8 presents the variation of the load flow between bus 6 and 12 considering the reduction in the maximum capacity of the main natural gas pipeline.

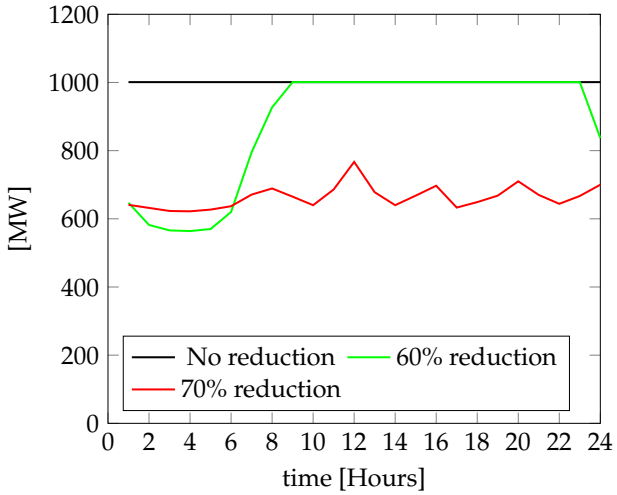

Figure 8. Variation of the load flow between bus 6 to 12 considering reduction of the maximum capacity of the main natural gas pipeline

3.5. Discussion

The results shed light on the implications of congestion in the natural gas network, particularly regarding system operating costs, bus prices, and power flow.

In scenarios where the maximum capacity of the primary natural gas pipeline is reduced by up to 50%, no significant variations are observed. Nevertheless, when reductions exceed 50% of the pipeline's maximum capacity, there is a noteworthy increase in energy production costs. These costs can escalate by as much as 69% in comparison to scenarios without congestion. Similarly, there is a significant increase in bus prices, often reaching their maximum values, accompanied by substantial fluctuations in load flows. In many instances, load flows approach or even exceed the maximum levels of transmission capacity.

Furthermore, the analysis uncovers that when congestion levels exceed roughly 70% of the pipeline's capacity, the results fail to converge. This phenomenon arises from a combination of factors, encompassing the installed capacity of the SEIN without gas generation, the constraints of transmission capacities, and the inherent limitations of network parameters. Consequently, it becomes imperative to implement load rejection systems to uphold system stability, as the system's demand cannot be met.

While the primary focus of this analysis is on natural gas pipeline congestion, it is important to note that similar hypotheses and results can be extrapolated to various other scenarios. These may include reduced natural gas supply, a gradual decline in natural gas production at the wellhead, diminishing proven reserves in the natural gas wells that supply the pipeline, and a range of other conditions.

4. Conclusions

This paper emphasizes the critical role of coordinating the electricity and natural gas markets to enhance operational efficiency and reduce associated costs, particularly in scenarios where pipeline co-management is involved.

The presented results provide valuable insights for shaping policies aimed at mitigating congestion effects in natural gas pipelines and addressing constraints in electrical

transmission. These findings emphasize the significance of improved coordination between both systems under a unified market operator.

The research demonstrates the effects of congestion scenarios on production costs in the gas–electricity system. Notably, scenarios with reductions in the maximum capacity of the main pipeline below 50% show no observable impact on energy production costs, bus prices, or load flows. However, when the reduction exceeds 50%, substantial increases in energy production costs, reaching up to 69% higher costs compared to congestion-free scenarios, are observed. Furthermore, reductions exceeding 70% in the maximum capacity of the main pipeline result in non-convergent results due to capacity limitations and network constraints, rendering the system unable to meet demand.

Finally, this paper identifies several areas that warrant further investigation in future research. These include the integration of additional natural gas sources, expansion of natural gas networks, incorporation of low-emission gases into the natural gas system, integration of renewable sources, deployment of flexible assets and operations, and the establishment of energy storage facilities. Addressing these aspects would require the inclusion of additional equations into the model.

Author Contributions: Conceptualization, R.N., H.R., J.E.L. and Y.P.M.; methodology, R.N. and H.R.; validation, J.E.L. and Y.P.M.; investigation, R.N. and H.R.; writing—review and editing, R.N., J.E.L. and Y.P.M.; visualization, J.L.S.; supervision, Y.P.M. All authors have read and agreed to the published version of the manuscript.

Funding: This research received no external funding.

Data Availability Statement: The original contributions presented in the study are included in the article, further inquiries can be directed to the corresponding author.

Acknowledgments: This research was supported by the Coordination for the Improvement of Higher Education Personnel (CAPES) through grant No. 1009/2024 and Process No. 88881.909446/2023-01, under the PRAPG Program. We thank the Faculty of Mechanical Engineering at the National University of Engineering, Lima, Peru, and the Department of Electrical Engineering at the Federal University of Paraíba, Brazil, for their indispensable support.

Conflicts of Interest: The authors declare no conflicts of interest.

Nomenclature

A	The electrical current flow measured in amperes (A)
AC	Alternating current
a_g, b_g, *and* c_g	These constants are integral to the quadratic equation used to compute the energy production cost from each bus generator. They vary based on the generator's power output and are denoted in [USD/MW2], [USD/MW], and [USD], respectively.
C_{Diesel}	The cost associated with generating electricity using diesel, expressed in [USD].
C_{rer}	The cost of generating electricity using both conventional and non-conventional renewable energy sources, in [USD].
C_{res}	Cost of energy storage system in [USD] that remains fixed throughout the period.
CDF	Conceptual data abstraction called Common Data Format for storing, manipulating, and accessing multidimensional datasets
C^2_{nm}	Constant dependent on the chemical structure of the NG, and the characteristics of the nm section of the NG duct ($m^6/bars^2$)
D_{nm}	Internal diameter of NG duct (mm)
δ_i	Voltage phase shift angle on bus i.
d_n	The demand for natural gas for non-electrical uses at node n, expressed in m^3/h or m^3/day.
e_n	The volume of natural gas flowing from node n to the generator, in m^3/s.

f_{mn}	The volume of natural gas transported from node m to node n, in m^3/h or m^3/day.
$f_{nm,max}$	The upper limit on the volume of natural gas flow from node n to node m, in m^3/h.
$f_{nm,min}$	The lower limit on the volume of natural gas flow from node n to node m, in m^3/h.
$f_{nm}(t)$	The flow of natural gas between nodes n and m during period t, measured in 10^6 m^3/h.
f_{no}	The volume of natural gas transported from Node n to Node o, in m^3/h or m^3/day.
Gen	The total number of power plants within the network.
$k1$	0.0023148 MWatts·day/106 m^3
LHV	Low Heating Value Constant equivalent to 35.07 MW/(m^3/s)
L_{nm}	NG pipeline length nm (km)
η	Thermal power plant efficiency
N	Bus number in the electrical network
NGs	Number of supply points in the NG network
P_{di}	The active power load on bus i during period t, measured in MW.
P_{GenBus}	The power generated at a bus, in MW.
PG	number of pipes in the gas network
p_g	Unit price of NG in [USD/m^3USD]
$P_g(t)$	Active Power delivered by the generator g in the period t in [MW].
P_{gi}	Power generated in MW by NG thermal plant
$P_{g,i}^{(t)}$	Variable Active Power delivered by the generator g on the bus i at time t in [MW]
PHI	Offset angle
P_{km}^{max}	Maximum limit of active power in the section k-m (MW))
P_{km}	Active Power in the section k-m (MW)
P_i	Active power on the bus i in the period t
P_L	Active power losses in period t
p_m	Pressure reached at node m (bars)
p_n	Pressure reached at node n (bars)
$p_{n,max}$	Maximum pressure limit at node n, (bars)
$p_{n,min}$	Minimum pressure limit at node n, (bars)
p_{tg}	Unit cost of NG transportation in [USD/m^3]
Q_{di}	Reactive Load on the bus i in the period t
Q_i	Reactive Power generated in bus i in the period t
Q_L	Reactive Power Losses in the period t
S_n	NG supply at node n in (m^3/h or m^3/day)
$S_{n,max}$	Maximum limit of the NG supply delivered by the producer or importer node n (m^3/h)
$S_{n,min}$	Minimum limit of the NG supply delivered by the producer or importer node n (m^3/h)
$S_n(t)$	Supply of NG supplied at node n in period t in [106 m^3/h]
T	Temperature constant of NG, 281.15 K
USD	US American Dollars
V	Volt unit of potential difference
$VFinBus$	Final bus voltage, p.u.
V_i	Bus voltage value i;
W	Power Unit in Watts
X	Electrical impedance
Y	Admittance
Y_{ij}	Impedance of the line between busbars i and j
z	compressibility factor of NG, 0.8 (dimensionalless)
δ	Density of NG with respect to air, 0.6106 (dimensionalless)
δ_i	Angle of the tension in bar i
ε	Absolute roughness of the NG duct, 0.05 mm
η	Efficiency of the thermoelectric plant
θ_{ij}	Angle of total line admittance between busbars i and bus j
$\sum_{i=1}^{N} P_{gi,t}$	Total energy generated on the bus i in the period t
$\sum_{i=1}^{N} P_{di,t}$	Total Active Energy in bus i in period t
$\sum_{i=1}^{N} Q_{gi,t}$	Total Reactive Energy in bus i in the period t

$\sum_{i=1}^{N} Q_{di,t}$	Reactive load on bus i in period t
$\sum_{g=1}^{G} P_{gi}$	Active Power of the thermogenerators connected on the bus i
$\sum_{g=1}^{G} Q_{gi}$	Total Reactive Power of the thermogenerators
z	NG compressibility factor, 0.8 (dimensionalless units)

Abbreviations

COES	Council for Electrical System Economy Operating
DNLP	Discrete Non-Linear Programming
GAMS	General Algebraic Modeling System
GW	Gigawatts
IEEE	International electrical and electronics engineers
Km	kilometers
KP	Key point
KV	Kilo volts
LNG	Liquefied natural gas
NG	Natural Gas
NGFTPUs	Natural-Gas-Fueled Thermoelectric Power Units
MMScm	Million Metric Standard Cubic Meters
MVA	Mega Volt-Amper
MW	Megawatts
SEIN	Peruvian National Interconnected System
SDDP	Stochastic Dual Dynamic Programming
NGFTPUs	Natural-Gas-Fueled Thermoelectric Power Units

References

1. Xing, J.; Wu, P. Optimal Planning of Electricity-Natural Gas Coupling System Considering Power to Gas Facilities. *Energies* **2021**, *14*, 3400. [CrossRef]
2. Saedi, I.; Mhanna, S.; Mancarella, P. Integrated electricity and gas system modelling with hydrogen injections and gas composition tracking. *Appl. Energy* **2021**, *303*, 117598. [CrossRef]
3. Ameli, H.; Qadrdan, M.; Strbac, G. Coordinated Operation of Gas and Electricity Systems for Flexibility Study. *Front. Energy Res.* **2021**, *8*, 17. [CrossRef]
4. Qin, G.; Yan, Q.; Kammen, D.M.; Shi, C.; Xu, C. Robust optimal dispatching of integrated electricity and gas system considering refined power-to-gas model under the dual carbon target. *J. Clean. Prod.* **2022**, *371*, 133451. [CrossRef]
5. AlHajri, I.; Ahmadian, A.; Elkamel, A. Techno-economic-environmental assessment of an integrated electricity and gas network in the presence of electric and hydrogen vehicles: A mixed-integer linear programming approach. *J. Clean. Prod.* **2021**, *319*, 128578. [CrossRef]
6. Rubio-Barros, R.; Ojeda-Esteybar, D.; Ano, O.; Vargas, A. Combined Operational Planning of Natural Gas and Electric Power Systems: State of the Art. In *Natural Gas*; Potocnik, P., Ed.; IntechOpen: Rijeka, Croatia, 2010; Chapter 12. [CrossRef]
7. Pambour, K.A.; Cakir Erdener, B.; Bolado-Lavin, R.; Dijkema, G.P.J. Development of a Simulation Framework for Analyzing Security of Supply in Integrated Gas and Electric Power Systems. *Appl. Sci.* **2017**, *7*, 47. [CrossRef]
8. Hibbard, P.J.; Schatzki, T. The Interdependence of Electricity and Natural Gas: Current Factors and Future Prospects. *Electr. J.* **2012**, *25*, 6–17. [CrossRef]
9. Ventosa, M.; Baillo, A.; Ramos, A.; Rivier, M. Electricity market modeling trends. *Energy Policy* **2005**, *33*, 897–913. [CrossRef]
10. Yang, L.; Zhao, X.; Li, X.; Feng, X.; Yan, W. An MILP-Based Optimal Power and Gas Flow in Electricity-gas Coupled Networks. *Energy Procedia* **2019**, *158*, 6399–6404. [CrossRef]
11. Navarro, R.; Rojas, H.; De Oliveira, I.S.; Luyo, J.E.; Molina, Y.P. Optimization Model for the Integration of the Electric System and Gas Network: Peruvian Case. *Energies* **2022**, *15*, 3847. [CrossRef]
12. Rojas, H. Despacho Integrado de Sistemas Eléctricos de Potencia y de Gas Natural considerando Energías Renovables y Sistemas de Almacenamiento. *Fondo Editor. UNI* **2022**, *1*, 147.
13. Jenkins, S.E. Interdependency of electricity and natural gas markets in the united states: A dynamic computational model. *Mass. Inst. Technol. Technol. Policy Program* **2014**, *1*, 84.
14. Erdener, B.C.; Pambour, K.A.; Lavin, R.B.; Dengiz, B. An integrated simulation model for analysing electricity and gas systems. *Int. J. Electr. Power Energy Syst.* **2014**, *61*, 410–420. [CrossRef]
15. Gil, M.; Dueñas, P.; Reneses, J. Electricity and Natural Gas Interdependency: Comparison of Two Methodologies for Coupling Large Market Models Within the European Regulatory Framework. *IEEE Trans. Power Syst.* **2016**, *31*, 361–369. [CrossRef]
16. De Wolf, D.; Smeers, Y. The Gas Transmission Problem Solved by an Extension of the Simplex Algorithm. *Manag. Sci.* **2000**, *46*, 1454–1465. [CrossRef]

17. An, S.; Li, Q.; Gedra, T. Natural gas and electricity optimal power flow. In Proceedings of the 2003 IEEE PES Transmission and Distribution Conference and Exposition (IEEE Cat. No.03CH37495), Dallas, TX, USA, 7–12 September 2003; Volume 1, pp. 138–143. [CrossRef]
18. Liu, C.; Shahidehpour, M.; Fu, Y.; Li, Z. Security-Constrained Unit Commitment with Natural Gas Transmission Constraints. *IEEE Trans. Power Syst.* **2009**, *24*, 1523–1536. [CrossRef]